Portable nitrous oxide sensor for understanding agricultural and soil emissions

Final Technical Report
Grant No. DE-SC0011288

Southwest Sciences, Inc.
1570 Pacheco St., Suite E-11
Santa Fe, NM 87505

Sponsoring Program Office: Office of Science, U. S. Department of Energy (SBIR)
Period of Performance: February 18, 2014 – January 17, 2017
Principal Investigator: Dr. Alan C. Stanton, Southwest Sciences, Inc.
Research Institution Investigator: Dr. Mark A. Zondlo, Princeton University

Research Team Members:

Southwest Sciences, Inc.

Dr. Alan C. Stanton, Principal Investigator (Principal Research Scientist)
Dr. Joel A. Silver, Principal Research Scientist
Dr. Anthony L. Gomez, Senior Research Scientist
Dr. Steven M. Massick, Principal Research Scientist
Dr. Mark E. Paige, Principal Research Scientist
Mr. Frank C. Carey, Research Engineer
Mr. Edwin Ochoa, Research Assistant

Princeton University

Dr. Mark A. Zondlo, Associate Professor of Civil and Environmental Engineering
Mr. Da Pan, Research Assistant
Mr. Levi Golston, Research Assistant
Mr. Lei Tao, Research Assistant

Acknowledgment: This material is based upon work supported by the Department of Energy [*Add Other Agencies, if applicable*] under Award Number DE-SC0011288.

Executive Summary

Nitrous oxide (N_2O) is the third most important greenhouse gas (GHG,) with an atmospheric lifetime of ~114 years and a global warming impact ~300 times greater than that of carbon dioxide. The main cause of nitrous oxide's atmospheric increase is anthropogenic emissions, and over 80% of the current global anthropogenic flux is related to agriculture, including associated land-use change. An accurate assessment of N_2O emissions from agriculture is vital not only for understanding the global N_2O balance and its impact on climate but also for designing crop systems with lower GHG emissions. Such assessments are currently hampered by the lack of instrumentation and methodologies to measure ecosystem-level fluxes at appropriate spatial and temporal scales.

Southwest Sciences and Princeton University are developing and testing new open-path eddy covariance instrumentation for continuous and fast (10 Hz) measurement of nitrous oxide emissions. An important advance, now being implemented, is the use of new mid-infrared laser sources that enable the development of exceptionally low power (<10 W) compact instrumentation that can be used even in remote sites lacking in power. The instrumentation will transform the ability to measure and understand ecosystem-level nitrous oxide fluxes.

The Phase II results included successful extended field testing of prototype flux instruments, based on quantum cascade lasers, in collaboration with Michigan State University. Results of these tests demonstrated a flux detection limit of 5 μg m^{-2} s^{-1} and showed excellent agreement and correlation with measurements using chamber techniques. Initial tests of an instrument using an interband cascade laser (ICL) were performed, verifying that an order of magnitude reduction in instrument power requirements can be realized. These results point toward future improvements and testing leading to introduction of a commercial open path instrument for N_2O flux measurements that is truly portable and cost-effective.

The technology developed on this project is especially groundbreaking as it could be widely applied across FLUXNET and AmeriFlux sites (>1200 worldwide) for direct measurements of N_2O exchange. The technology can be more broadly applied to gas monitoring requirements in industry, environmental monitoring, health and safety, etc.

Table of Contents

1. Introduction

1.1 Overview

Southwest Sciences, Inc., in collaboration with Prof. Mark Zondlo of Princeton University, is developing an open-path, eddy covariance nitrous oxide (N_2O) analyzer that is fast, sensitive, low power, lightweight, and robust enough for long-term field operation. The innovation is based upon novel advances in mid-infrared lasers, optomechanics, and open-path, mid-infrared detection schemes.

Our work in the initial Phase II project has focused on field measurements using prototype instrumentation to validate the open path measurement approach, coupled with investigation of new infrared lasers (interband cascade lasers) that offer the opportunity to dramatically reduce the size, weight, and most importantly, power requirements of the open path instrument. These lasers have become available at the requisite infrared wavelengths only during the past year. During Phase II, we have been able to demonstrate that the ICLs perform at a level that enables this dramatic improvement in field portability for N_2O flux instrumentation.

Nitrous oxide is an important greenhouse gas [IPCC, 2007] and dominant ozone depleting substance [Ravishankara *et al.*, 2009], and its emissions to the atmosphere are extremely heterogeneous in space and time [Reay *et al.*, 2012]. Novel approaches to characterize such heterogeneity and identify effective mitigation strategies are greatly needed. FLUXNET (http://fluxnet.ornl.gov) sites, as shown in Fig. 1, have dramatically improved the understanding of carbon land-atmosphere-biosphere exchange [Baldocchi *et al.,* 2001], and a similar network of N_2O eddy covariance tower measurements would greatly aid the understanding of the nitrogen cycle. The National Academy of Engineering lists the management of the nitrogen cycle as one of the grand challenges for engineering in the 21st century. (http://www.engineeringchallenges.org/cms/8996.aspx)

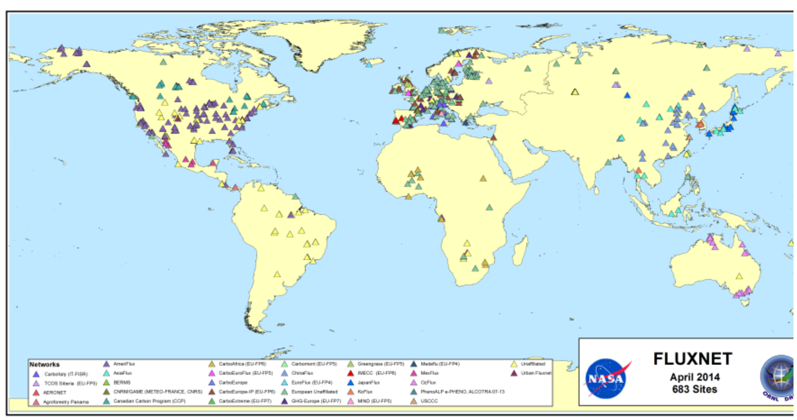

Fig. 1: Over 500 FLUXNET sites exist worldwide for understanding carbon/energy fluxes. The N_2O instrument in this network will be useful for the nitrogen cycle.

The instrument development in this project will allow for researchers, regulators, and environmental consultants to accurately and effectively measure N_2O emissions at unprecedented spatial and temporal scales in a quick, efficient, and easy manner. Customers who use the sensor will be able to make new discoveries for publications, promotion, and prestige for researchers, to identify effective environmental regulatory actions for government policy makers, and to lower labor and field costs for improved profits for environmental consultants.

1.2 Background and Significance of the Innovation

Nitrous oxide is the third most important anthropogenic greenhouse gas (GHG) with an atmospheric lifetime of ~120 years and a global warming impact ~300 times greater than that of CO_2 on a per molecule basis [IPCC, 2007]. The atmospheric increase of N_2O is mostly due to anthropogenic emissions related to agriculture, and ~50% of the total anthropogenic flux is emitted from agricultural soils [Reay *et al.*, 2012]. Global N_2O emissions are expected to increase 20% through land use change and agricultural intensification (in particular fertilizer use) by 2030 [Vitousek *et al.*, 2009; Smith *et al.* 2012]. An accurate assessment of N_2O emissions from agriculture and natural soils is therefore vital not only for understanding the global N_2O balance and its impact on climate, but also for designing cropping and other systems with lower greenhouse gas emissions. Currently hampering this effort is the lack of methodologies to measure ecosystem-level fluxes at appropriate spatial and temporal scales [Butterbach-Bahl *et al.*, 2013].

The current "state of the art" method for measuring soil N_2O emissions is the static chamber method, which was developed in the 1980s and is still used widely around the world [e.g. Holland *et al.* 1999; Butterbach-Bahl *et al.* 2013]. The method is relatively simple, which is part of its power: an open-bottomed, gas-tight box is placed over an area of soil and over the course of ~60 minutes, the accumulation of headspace N_2O is measured. With proper care and replication, the rate of accumulation of headspace gas can be extrapolated to an approximate ecosystem flux. However, there are three well-known limitations with this method: 1) chambers cover only a very small area (typically ~0.25 m^2); 2) they do not account for emissions for those parts not covered by the chamber (e.g. leaves, tree canopies); and 3) they cannot be sampled continuously without significant, expensive and power hungry automated systems. As a result, measurements of soil N_2O emissions are usually performed with very low temporal and spatial resolution. Soil N_2O emissions, however, are known to have very high spatial and temporal variability, and are often characterized by high episodic fluxes [e.g. Ruan and Robertson, 2013]. The resulting uncertainty (high measurement variance) proliferates through higher-level extrapolations, making it difficult to identify any but the largest treatment and ecosystem differences in experimental settings and difficult to estimate regional and global N_2O fluxes with certainty. This creates a major knowledge gap.

The shortcomings of static chamber methodologies are well-known, and past efforts to develop micrometeorological techniques, which have been transformative for our understanding of ecosystem C fluxes [e.g. Piao *et al.* 2008; Migliavacca *et al.* 2011; Schwalm *et al.* 2012], have met with mixed success for N_2O. For CO_2, the eddy-covariance (EC) approach is now used world-wide with open-path sensors to estimate CO_2, water, and energy fluxes (http://fluxnet.ornl.gov/). The current work anticipates a similar network of N_2O sensors as part of ecological and flux networks, as is currently being done with CO_2.

For N_2O, current best EC approaches require closed-path analyzers, which consume large amounts of power (500-1000 W) and are relatively insensitive [Neftel *et al.* 2010; Zona *et al.* 2012]. In a closed path system, gas is pumped from a position above the plant canopy to a ground-based shed that houses an instrument connected to line power. Closed path systems have illustrated the power of EC approaches for N_2O [Zona *et al.* 2012, 2013], but their applicability for field use is limited by the need for grid power and the inherent size/mass of closed-path analysis. There is no robust technique for continuously measuring ecosystem-level N_2O emissions with high-precision, especially at remote locations [e.g. Hensen *et al.* 2013].

The work we are pursuing here will advance the development of a new open-path, eddy covariance technique for N_2O. We are using state-of-the-art mid-infrared technologies including interband cascade lasers, compact optomechanical configurations [Silver, 2005], new detection schemes for field stability under changing conditions [Tao *et al.*, 2012; Sun *et al.*, 2012; Sun *et al.*, 2013], and proprietary software and electronics. Interband or quantum cascade lasers probe the fundamental (most sensitive) N_2O absorption band in the mid-infrared spectral region near 4.54 μm and offer significant improvements in sensitivity and instrument size. These new lasers are undergoing rapid progress in their thermal and optomechanical packaging, output power, current tuning ranges and capabilities to be modulated for high sensitivity detection schemes such as wavelength modulation spectroscopy (WMS), and field robustness.

The groundbreaking nitrous oxide instrumentation under development in this project will transform the ability of atmospheric researchers to measure and understand ecosystem-level N_2O fluxes at multiple scales. The instrumentation will provide an experimental capacity to understand fundamental patterns and controls of this important greenhouse gas at the ecosystem scale.

2. Project Objectives

The Phase II objectives were to build, field test and validate, and demonstrate the analyzer. Specific Phase II objectives are noted below, along with a brief statement of status at the end of Phase II:

Task I: Design an alpha prototype

Status at completion of project: An alpha prototype unit was designed, assembled, and tested at Southwest Sciences.

Task 2: Quantify methods to reduce uncertainties in N_2O flux measurements

Status at completion of project: This task was performed at Princeton, and emphasized improved understanding of spectroscopic effects on the measurements.

Task 3: Understand how the sensor design impacts the measurement

Status at completion of project: These tests, which were to be conducted at Princeton University using wind tunnel facilities, were deferred in favor of more extended field testing of alpha and beta prototypes during the project.

Task 4: Evaluate how temperature cycling impacts the sensor performance

Status at completion of project: System drift on the prototypes was studied extensively at Southwest Sciences, and factors different from environmental temperature were identified that dominated system drift. These results are discussed below.

Task 5: Test system performance in the field

Status at completion of project: Extensive field tests of the prototype instruments were conducted by the Princeton group in both years of the Phase II project, as discussed below.

Task 6: Develop custom electronics that are stable and precise

Status at completion of project: Custom electronics were developed and tested at Southwest Sciences, and incorporated into prototype systems, as described below.

Task 7: Develop user-friendly software with appropriate diagnostic parameters

Status at completion of project: LabView software to provide user interfacing and control of the system was developed at Southwest Sciences.

Task 8: Construct a beta-prototype unit

Status at completion of project: Our work in constructing a beta prototype took a direction not anticipated at the start of the project, as new lasers (interband cascade lasers) became commercially available that have significant operational advantages for field instrumentation. We directed our efforts in the latter stages of the project at establishing that these lasers could be effectively used, instead of power-hungry quantum cascade lasers, in constructing future versions of the field instruments.

Task 9: Demonstrate long-term performance in the field

Status at completion of project: Long-term field testing was conducted by Mark Zondlo's group at Princeton, and results of these tests are described in this report.

3. Project Accomplishments and Results

3.1 Overview

The Phase II efforts were approached from two coordinated directions: (1) software and electronics development, and mechanical design at Southwest Sciences in a controlled laboratory setting for developing a field worthy system; and (2) refining of the science aspects for making useful field measurements and calculations of N_2O fluxes using a second QCL N_2O system at Princeton University which was based on an older, unrefined, high power design. During the second half of Phase II, we studied the use of a recently introduced interband cascade laser (ICL) operating at 4.5 µm as an alternative to the original quantum cascade laser (QCL). The ICL had the huge benefit of operating at substantially lower power. As a result, the final hardware design was redirected (Table 1).

Table1: Physical specifications comparing the ICL and QCL systems developed at SWS.

	QCL	**ICL**
Weight (optical head)	4.3 lb	5 lb*
Weight (electronics box)	17.7 lb	N/A
Size (optical head)	23.5 x 5.75 x 3.5 (in)	30 x 6 x 4 (in) *
Size (electronics box)	16 x 12 x 5.25 (in)	Not needed
Laser Input Power (excl. TEC)	2.5	0.1 to 0.2 watts
Total System Power	30 to 50 watts	6 to 9 watts
Optical head cooling	Liquid closed loop	Not needed
Electronics cooling	Fans	N/A
Laser driver	External + DSP	Integrated with DSP board
TEC control	External + DSP, x2	Integrated with DSP board

*estimated since the ICL based enclosure and PCB layouts would be redesigned in future work.

3.2 Instrument Design

System Overview:

The N_2O flux instrument is composed of two main units, a compact optical head, and a remote electronics module. These units were designed specifically for outdoor use. Sensitive electronics are housed in low solar absorption NEMA 4X weather tight enclosures. Electronic feedthroughs were specifically chosen to ensure a water tight seal. These two units are connected by a detachable 10 ft umbilical cable. The bundle is protected from abrasion with a braided nylon jacket.

Optical Head:

The core of the optical head is a 20 meter cylindrical mirror multipass cell. The SWS patented dense pattern cell has better aperture clearance (reducing unwanted etalon effects) when compared to a traditional Herriott cell of equivalent path length. The multipass cell is built using carbon fiber rods that have low coefficients of thermal expansion (~2 ppm/°C). The 8 mm carbon rods have significantly higher stiffness and greater damping than previously used low-thermal-expansion invar rods. The optical mounts are all lockable, and the flexure mount used for the input mirror has less thermal walk than traditional mirror mounts. The cell mirrors have resistive heating elements to prevent frosting and condensation. This optical rail system is insulated from the sealed optical platform with a Teflon spacer to limit thermal transfer. The QCL version required greater thermal control to minimize thermal drift and used a closed-loop liquid cooler housed in the remote electronics box (the ICL version had this sub-system removed). The laser and detector are thermally stabilized with TEC controllers and are mounted to a common metal plate along with the steering optics. Steering optics use top adjusting miniature flexure mounts for thermal stability. A small fan (not needed with the ICL) is housed inside the sealed optical head to maintain temperature uniformity. A 532 nm co-alignment laser is installed to allow easy re-alignment should optics get nudged out of alignment. The detector is a Hamamatsu InAsSb diode run in photovoltaic mode (no bias),

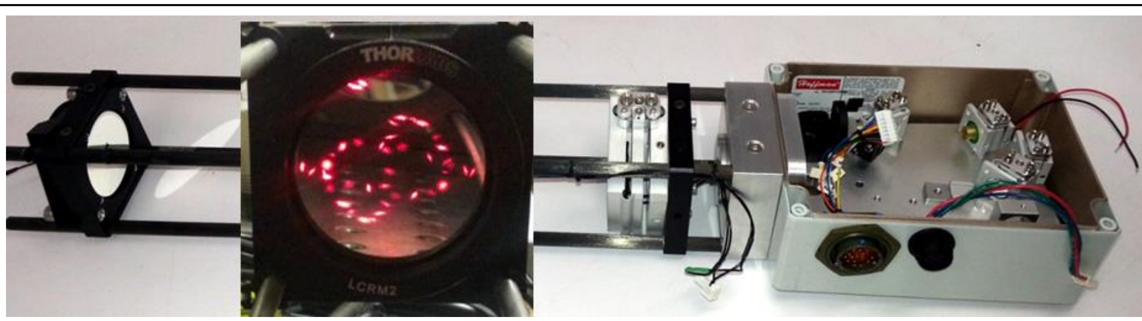

Figure 2: Phase II optical head with pre-amp/interface board removed for clarity. Cylindrical cell spot pattern using alignment laser shown as inset.

having a custom anti-reflective coated window to minimize etalon interference. The detector signal is amplified in the optical head with a transimpedence amplifier to ~1 V to minimize signal degradation through the umbilical.

Lasers:

The original system was designed with a QCL in mind and was later adapted to an ICL due to significant power (and optical) advantages. We evaluated QCL lasers from Adtech, Hamamatsu and Corning. These power hungry lasers had a lasing threshold ranging from 150 mA up to almost 1 A and a compliance voltage of 11 – 12 V. Our final QCL choice was by Corning as it had the best integrated lens system, appropriate beam diameter, and lowest power requirement of the QCLs. However, it still required 2.5 watts just for the laser, and almost 10 times as much power was required just to cool the laser with the TEC, plus additional power to transfer the heat away from the optical head with the liquid cooling system. We later changed to a NanoPlus ICL which behaved more like a traditional telecom DFB laser than a QCL. Its lasing threshold was only 35 mA with a compliance voltage of under 2 V. The total power required to run the ICL (including its TEC) was just over 1 watt! This incredible power reduction allowed us to significantly simplify our electronics design at the second half of Phase II.

Although the ICL required external optics, it had additional advantages as compared to the QCL with integrated optics. QCLs have very divergent and asymmetrical beam profiles. This can cause etalon effects when the divergence of the laser exceeds the numerical aperture of the collimating optic. The QCL also had a "standard" AR-AR coating. By using our own lens, we were able to better match the divergence (significantly lower with the Nanoplus ICL) and focal length to the system, allowing us to put the beam waist at the desired location within the multipass cell. We also were able to use a custom high performance narrow band AR-AR coating to further reduce etalon fringing.

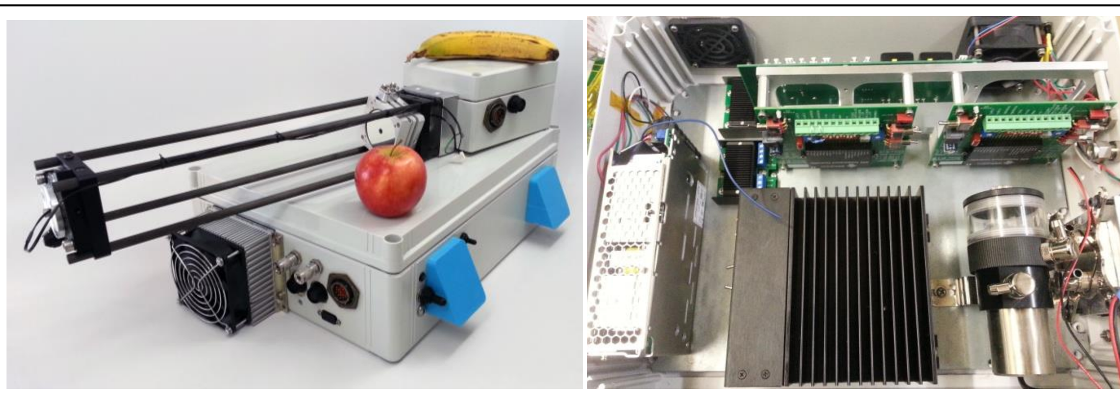

Figure 3: (Left) completed optical head sitting on QCL electronics box. (right) Inside of the QCL version of the electronics box (SWS DSP board is not installed) showing the hardware required for sufficient temperature regulation and power. The revised system based on the ICL would not need many of these subsystems, allowing all electronics to be moved to the optical head while still preserving the small wind shadow foot print of the original optical head design.

Electronics:

The heart of the instrument is a Southwest Sciences designed DSP board (Fig 4, top) which controls all aspects of the system. The board operates at 300 kHz, producing a 250 kHz modulation and 1.5 kHz ramp rates for WMS detection. Lock -in detection, AC/DC amplification, and filtering are all performed with analog circuitry. ADCs are used to input the signals into the DSP. The DSP and additional digital electronics run custom code which handles laser current and laser TEC control, on-the-fly SVD data computations, and acquires the pressure (in the electronics box) and temperature (external to optics box) for mixing ratio corrections. The board then outputs the measured N_2O number density at 20 Hz via RS232, along with pressure and temperature (for calculating mole fraction) and additional diagnostic and instrument health information.

Since the ICL had low current and voltage requirements, the SWS board was able to directly drive the laser current and TEC current. The QCL however, required external electronics (Fig. 3). For the QCL, the SWS board was modified to output voltage signals to control a Wavelength Electronics QCL driver and TEC controller.

The original system had both AC and 12 V DC input power options to handle the power hungry QCL and related subsystems. A power distribution/conversion board (Fig. 4 bottom) was built to power the subsystems and had the circuitry for pressure measurements and RS232 I/O. The low noise amplifiers were optimally operated at 3.3 V, the SWS board at 6 V, the original TEC drivers for the QCL, detector, and cooling at 12 V. Lastly the Wavelength Electronics QCL laser driver required +/- 24V. By replacing the QCL with the ICL, we were able to remove the +/- 24V DC-DC converters and remove the need for AC. The ICL system ran at a total of 6 to 9 watts (depending on ambient temperature), which is easily powered long term in the field with solar cells and integrated battery reserve.

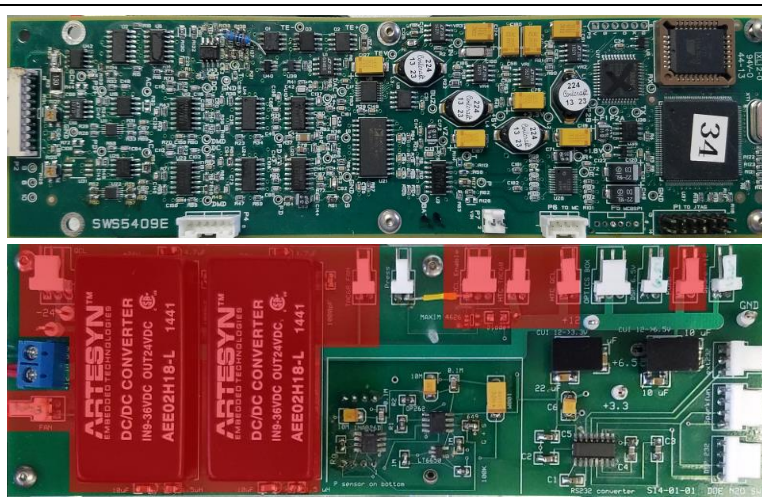

Figure 4: (Top) SWS DSP and analog electronics which controls the entire ICL based N_2O system. (Bottom) Power conversion, pressure measurements, and RS232 I/O. The red portions are not needed for the ICL system.

Since the QCL had such a high heat load, a closed loop liquid cooler located in the electronics box was used to export heat out of the optical head. This cooler used a large TEC, heatsink and fan. The QCL electronics box also had a high heat load with the controllers and subsystems and used an environmentally shielded fan to duct in cooling air. With the change to the ICL, the liquid cooling lines, pump, large TEC, and fan were removed. A future redesign would allow the DSP and power board to be relocated into an elongated optical head, removing the need for a separate electronics box.

3.3 Laboratory Measurements

Experimental Conditions:

Development of the QCL and ICL prototype systems was performed under laboratory conditions to optimize performance, perform calibrations, and determine system performance and pathways for improvements in a controlled environment. The following results will focus on the ICL based design.

Measurements were performed under sealed and open conditions. Sealed measurements were performed by putting the optical head in an 8" diameter steel vacuum tube having gas and hermetically sealed electrical feedthroughs. This allowed us to control mixing ratio, vary temperature using heating tape, and change pressure with a vacuum pump. When the gas ports were opened, we could fix temperature and mixing ratio while varying temperature. Cylinders of compressed whole air, N_2O calibration gas, and N_2 purge gas were available for testing and calibration. Unsealed measurements were performed fully open (to sample lab air) in which temperature, pressure and mixing ratio could freely change, and semi-open in which a shroud was placed over the optical arm to allow temperature and pressure to freely change while maintaining mixing ratios.

Data Acquisition and Fitting:

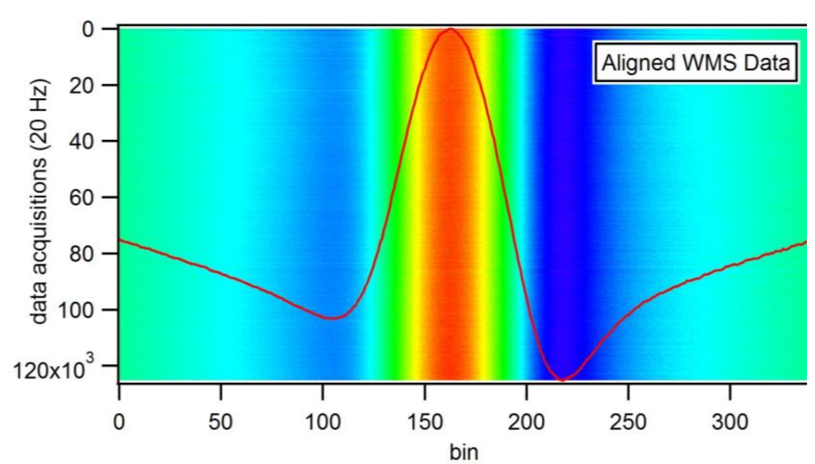

Figure 5: Example of 100 minutes of data taken with external NI DAQ system show in 2D image representation. The red trace is the basis vector for SVD fitting. Distortion in the WMS waveform is due to faster than optimal modulation with the stock DSP clock.

The electronics were designed to allow for parallel measurements and calculations for diagnostics, troubleshooting, and optimization. In addition to the self contained DSP data processing, analog signals were available for an external National Instruments DAQ for logging on a custom Labview program (Fig. 5). This allowed greater flexibility in post process analysis which would help identify areas for future improvement.

The DSP board is self contained and does all analysis on the fly without the need to store raw data. AC and DC digital inputs were sampled alternately point by point at 300 kHz and directly ratioed for normalization. Waveforms were acquired at 100 Hz and were co-averaged to 20 Hz. The resulting data were fit against a stored basis spectrum. Temperature corrections were made from Hitran cross sections, using temperature data obtained from the thermistor on the optical head. For the narrow range of operating pressures, empirical fit corrections were determined using a micro pressure gauge on the power distribution board. Alternatively, we could use a T/P correction look-up table and fit the data trough-to-trough with bin scaling. We have previously done such corrections with high levels of accuracy for measuring O_2, CO_2, CH_4, and H_2O.

Precision Limits and Improvements:

Although the QCL system at Princeton and ICL system at SWS were optically very similar, there was a difference in precision that needed to be addressed. Systematic studies on the ICL system identified three areas that limited the precision of the measurement, each spanning different time domains. We determined that each of these precision limits can be mitigated in future work. Allan variance analysis shows that the system is effectively "white noise" limited until around 10 seconds. At 10 Hz, the precision is 0.3 ppb or 1 part in 1083. Precision gains with "white noise" reduction or averaging go away at around 10 seconds. Precision levels off to around 0.1 ppb (1 part in 3250) at over 15 minutes (Fig. 6).

For short integration times (on the order of a second or less), precision is not limited by signal strength or detector noise, but rather by how we adapted the DSP board to run slower than its native ramp rate. In essence, rather than a smooth ramp, the laser stepped and held at fixed currents to coaverage. This resulted in ~1.5 kHz ripple in both AC and DC (the native ramp rate of the system). Because of the multiplex acquisition, the ripple is phase shifted between AC and DC and can't be removed by ratioing but is improved with averaging because it is asynchronous with the ramp. A revision of the DSP board and code will allow for smooth 100 to 200 Hz ramping. Additionally,

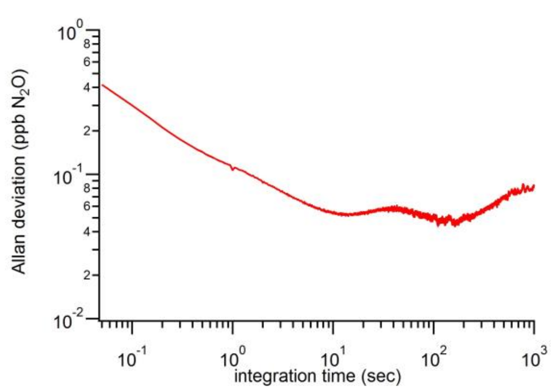

Figure 6: Allan deviation plot showing precision of overnight measurement using DSP for data analysis.

there is some A/D and D/A switching noise on the DSP board that is mostly removed through filtering, but may have some contribution to noise at these precision levels. Further circuitry refinement would solve this possible issue with the DSP. For medium integration times (a few seconds), drift is related to laser line locking and fitting. This can be seen when we compare N_2O concentrations directly to the laser TEC temperature. In short, a combination of bit resolution, and bin resolution, along with slight TEC overshoot causes the WMS peak to slightly drift. An increase in bin acquisitions and a more robust line locking/fitting algorithm should solve this mid term drift.

Long term drift is largely dominated by phase drift. WMS measurements require system phase to remain constant. Quadrature detection doesn't eliminate phase drift in WMS because of the out of phase component of the signal. Mid IR detectors have a very low shunt resistance at around a few ohms at room temperature for a 1 mm detector. This causes both the responsivity and phase of the detector to change depending on which portion of the surface is illuminated. The responsivity can be accounted for by ratioing AC to DC but the phase error would persist. In this work, we used a 1 mm Hamamatsu InAsSb detector. When phase error due to the detector was identified, we made efforts to better regulate the detector temperature at a low temperature. We were able to increase the shunt resistance by a factor of 10 by operating the detector TEC at -30°C and, as a result, we saw reduction in phase related drift as the laser moved across the detector by a similar amount. Over-filling the detector helped to some extent, but introduced unwanted etalon fringes. In future work, we will use a 3 stage TEC cooled detector which operates at -60 °C. Additionally, it uses a much smaller physical chip that is optically immersed to effectively act as a larger area detector. Since the shunt resistance is inversely proportional to the area, phase drift would go down substantially. The Vigo PVI-3TE-5 (effective 0.5 x 0.5 mm) detector with optical immersion and 3 stage TEC has a shunt resistance of 12 kohms, or ~1000x higher than the Hamamatsu detector at -30 °C.

Currently, the single board computer system at Princeton has advantages with precision in the ~1 second and faster integration times. However, this has been attributed through systematic studies to the SWS DSP running non-optimally so that it could be used to operate ICL and QCLs which run much better at slower ramp and modulation rates. Revision of the DSP boards should normalize the discrepancy such that the ICL system will have ~ 0.1 ppbv precision at 10 Hz rather than the current 0.3 ppbv precision. Additionally, with the goal of a lower power system, it is worth noting that the single board computer requires ~ 5 watts of power to run, while the DSP runs on about 1 – 200 mW (excluding laser and TEC stages which are not present on the single board computer).

3.4 Summary of Field Results

The Phase II project involved extensive field testing by the Zondlo group at Princeton University using a QCL-based prototype eddy covariance system at various stages of development, providing real-time feedback to Southwest Sciences to continuously improve the final ICL (and earlier QCL) based sensor design and identify field performance issues during the project. An open-path N_2O sensor was deployed in the field for over 50% of the 24 month Phase II project. This field testing strategy provided more 'real world' feedback than the originally proposed short-term deployments (weeks) scattered about the project, followed by a longer field testing design (months) near the end. For example, the thermal management of a sensor (laser/detector temperature stability and optomechanical alignment) could be examined over a range of temperatures from spring through autumn, as opposed to several shorter (few week) deployments with limited temperature ranges. Furthermore, optical degradation of exposed surfaces could also be studied in this more lengthy field testing strategy.

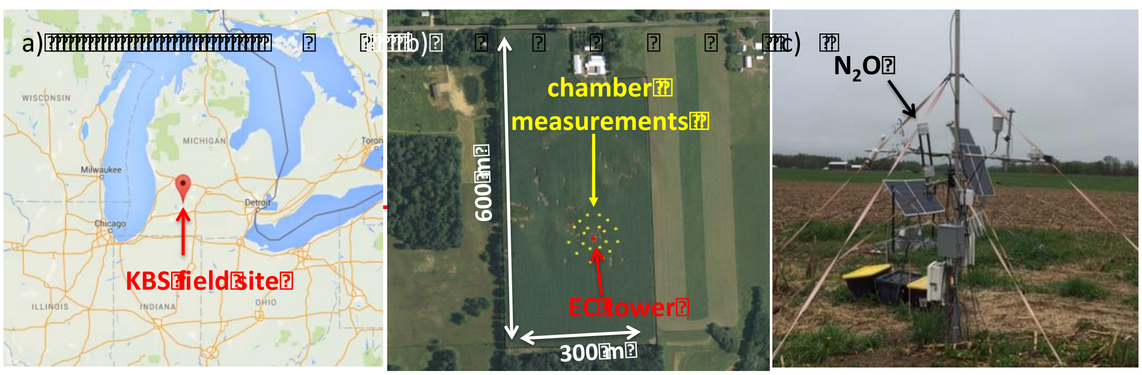

Figure 7: Field testing site a) Kellogg Biological Station at Michigan State University; b) aerial view of the corn field showing the tower site (red dot) surrounded by the flux chambers (yellow); and c) photograph of the solar-powered tower with a sonic anemometer, LICOR H_2O and CO_2, and eddy covariance N_2O sensor.

In both 2015 and 2016, prototype versions of the N_2O sensors were deployed on a tower in an experimental corn field managed by Kellogg Biological Station (KBS) to measure N_2O fluxes. We collaborated with Prof. Phil Robertson and Dr. Illya Gelfand of Michigan State University (MSU) for the field testing at this site. The site is particularly advantageous because it also contains a series of flux chambers around the footprint of the tower to help intercompare the EC fluxes with those measured from the chambers. Figure 7 shows the location of the (a) KBS site in Michigan, (b) the 600 $\times$ 300 m corn field managed by MSU with the locations of the chambers around the tower footprint, and (c) a photograph of the tower and sensors shortly after planting.

The 2015 and 2016 deployments lasted from May to October. At this site, herbicide is usually applied in early May followed by seeding, and fertilization occurs in mid-June. There were measurements of wind velocities (from CSAT3 sonic anemometer) and CO_2 and H_2O concentration (from LI7500) on the tower. The tower was raised every several weeks to maintain proper measurement heights (~ 2 m) above the growing corn canopy. The entire system was powered by two solar panels in the field. The sensors consumed between 45-60 W of power.

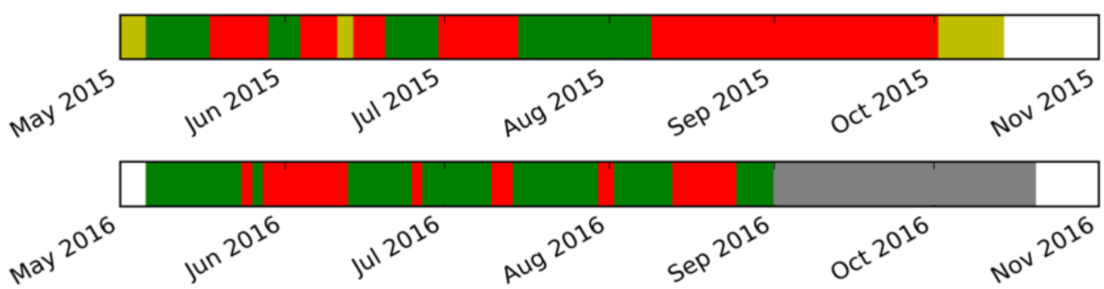

Figure 8: Operational status of the EC N_2O sensor for 2015 and 2016, showing the improvement from year-to-year. Green areas indicate fully operational sensor, yellow indicates the sensor is operational but at somewhat lower precision, and red indicates sensor malfunction or off-line. The gray area after September 2016 is where measurements were conducted but full QC/QA is currently underway for the micrometeorological data. Data dropouts were due to detector issues in 2015 and due to solar power supply voltage/sensor restart issues largely in 2016. Routine maintenance of cleaning of the mirrors occurred on average once every week or two.

Overall, the sensor worked properly for 34% and 59% of the time in 2015 and 2016, respectively. Fig. 8 shows the operational status of the sensor for each deployment. In 2015, a large fraction of missing data resulted from problems with the detector thermal control and lack of anti-reflection coatings on the windows from the detector manufacturer (Judson) that caused optical fringing. The detector problem was resolved in 2016 by using a custom anti-reflectivity-coated window on the detector (Intelligent Materials Solutions, Inc.).

In 2016, the downtime was mostly caused by an unstable battery/solar power supply. To prevent damage of the laser and detector, the EC N_2O system shut down when the voltage level dropped below 12 VDC. There was no mechanism to automatically restart the program when voltage levels increased back to normal. Other downtimes in 2016 were related to operational aspects such as calibrations in the field, mirror cleaning, and sensor cleaning.

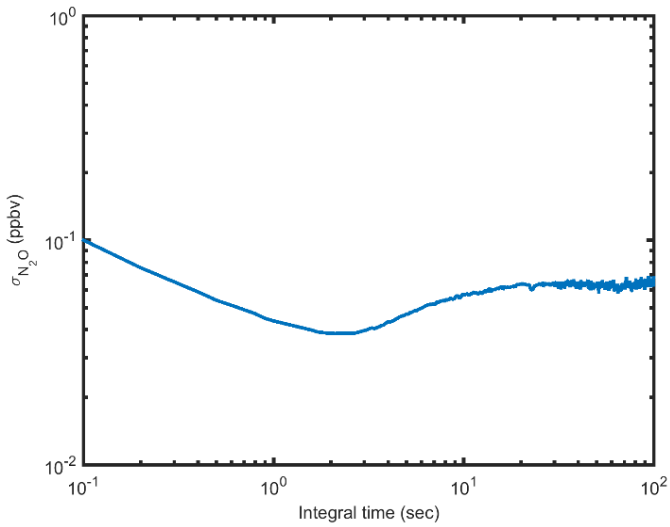

Figure 9: Allan deviation plot for the field-based sensor in 2015. A precision of 0.1 ppbv at 10 Hz N_2O was achieved with good stability.

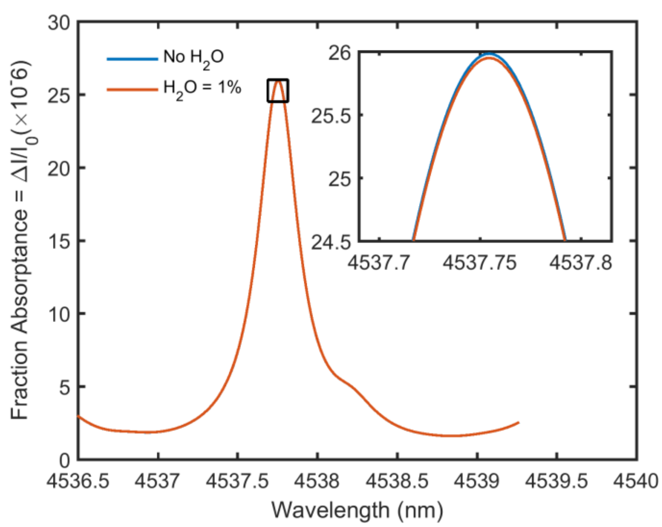

Figure 10: Water vapor broadening effects for a change of 1% absolute in water vapor mole fractions. This effect caused an effective decrease of -0.4 ppbv on the retrieved N_2O signal height.

Figure 9 shows an Allan plot of the sensor in the field prior to fertilization and during stable conditions when atmospheric fluxes should be minimized. The precision of the sensor at 10 Hz was 0.1 ppbv N_2O, and it remained below this drift for at least 5 minutes.

Before calculating fluxes, spectroscopic effects on the retrieved N_2O concentrations from variations of temperature, pressure, and water vapor concentration were conducted. Laboratory experiments at Princeton were conducted to measure the H_2O broadening coefficient on this absorption line of N_2O. Figure 10 shows the differences in 2f spectra taken with no H_2O and 10,000 ppmv H_2O. The H_2O broadening coefficient in the laboratory was measured to be 0.084 ± 0.06 cm^{-1} atm^{-1}, in good agreement with the literature for nearby absorption lines. Effectively, this means that an increase of 1% H_2O (e.g. 10,000 ppmv to 20,000 ppmv) requires correcting the N_2O mixing ratio by +0.4 ppbv N_2O. Because water vapor variations rarely reach this level at short timescales (10 Hz to 30 minutes), the broadening corrections are usually fairly negligible.

After correcting for spectroscopic effects, a Python-based program was developed to calculate the flux over a 30-minute window from the 10 Hz raw data. The calculation procedure follows that of EddyPro software (6.0.0, LI-COR Biosciences, Inc., NE), including flux corrections for low- and high-pass filtering and WPL density effects. WPL corrections terms accounted for about 54% of the total flux. In addition, a stationary test was conducted over a 30 minute period as well as a well-developed turbulence test (u*>0.1 m s^{-1}). Finally, the footprint had to be within 150 m of the tower (footprint defined as the upwind distance capturing 70% of the flux). As is typical for eddy covariance techniques, these criteria filtered out most (but not all) flux measurements during the night.

Figure 11 shows a time series of measured ambient temperatures and relative humidities (a), sensible heat fluxes and latent heat fluxes (b), N_2O and CO_2 mixing ratios (c), N_2O fluxes and N_2O fluxes before applying WPL corrections (the largest correction term, panel d) for a portion of 2016 several weeks after fertilization. Only flux results with valid meteorological conditions as described above are shown in Fig. 11. The N_2O mixing ratios during daytime approach regional background levels of ~ 326 ppbv N_2O but increase rapidly during nighttime as small emissions get trapped in the boundary layer. Daytime emissions are generally well-mixed

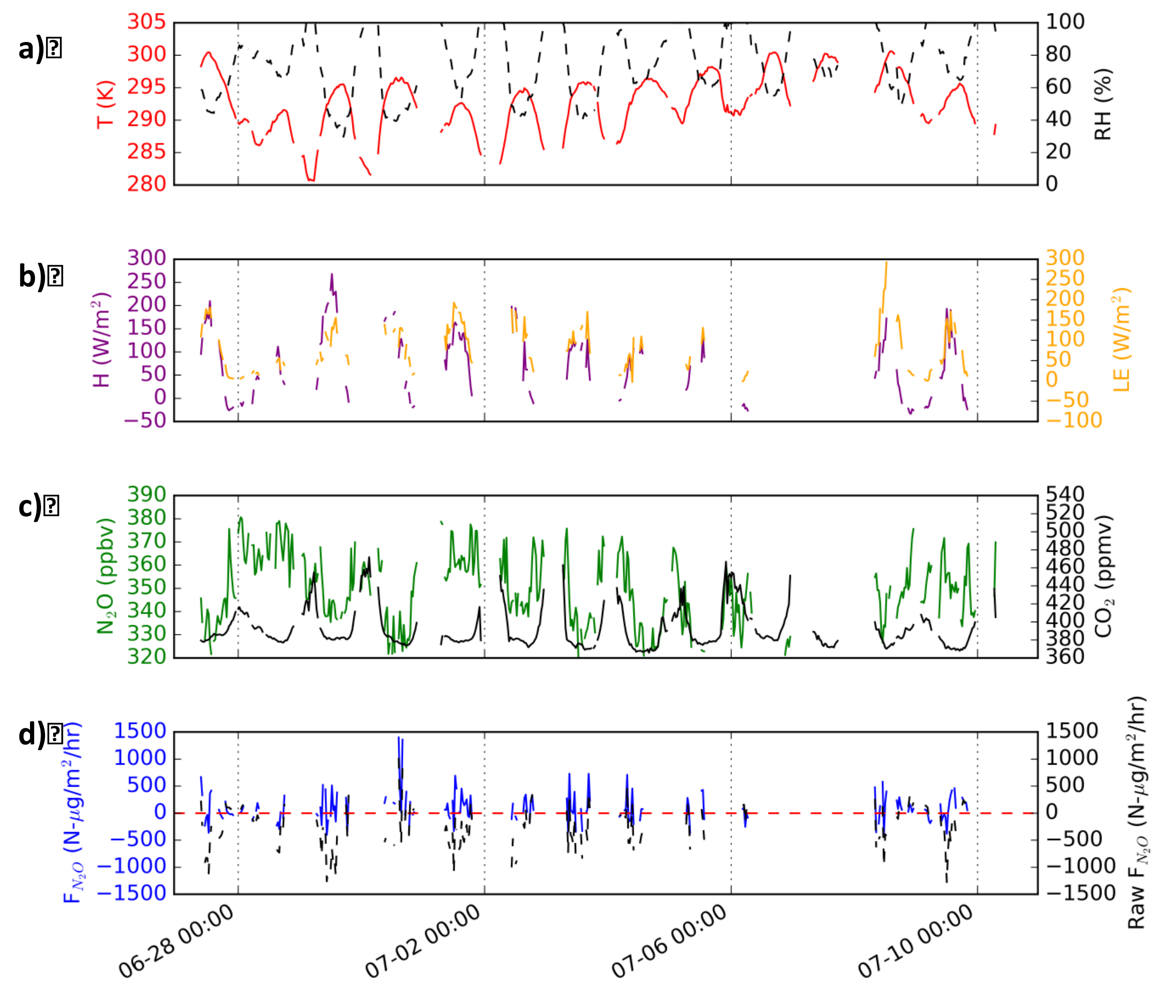

Figure 11: Time series of raw and processed data for (a) temperature and relative humidity, (b) sensible and latent heat fluxes, (c) N_2O and CO_2 mixing ratios, and (d) corrected and uncorrected N_2O fluxes.

with "cleaner" air to prevent large mixing ratios during daytime, though they are still often elevated above background levels. Similar night behavior is observed for CO_2 (emissions from respiration and lowering of the boundary layer at night), though CO_2 is taken up by the corn during daytime (opposite of N_2O emissions during daytime). Overall, significant day-to-day and diurnal variations are observed in the N_2O fluxes.

Figure 12 shows the co-spectra of N_2O and temperature in stable and unstable conditions. Corrections were made to account for the differences in location between the two sensors. Both scalars should show similar behavior and approach -4/3 slope at high frequencies (shown by black line). No significant differences are noted indicating that the fluctuations measured in the N_2O sensor are caused by atmospheric turbulence and not instrumental noise.

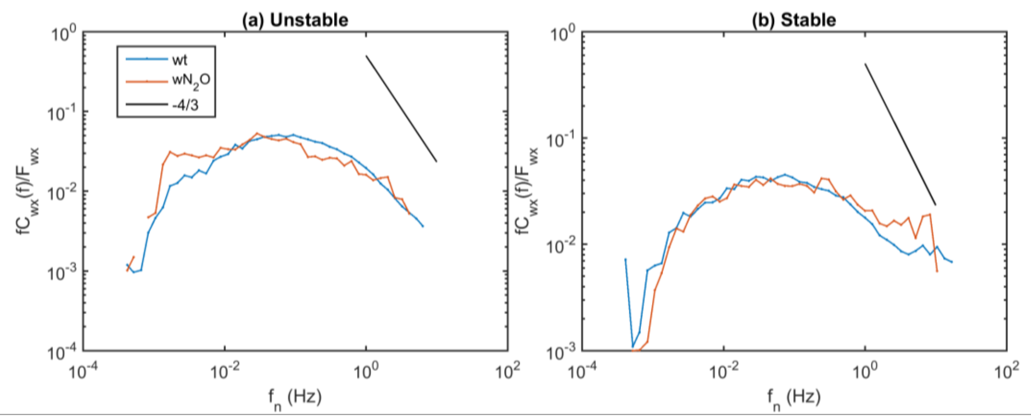

Figure 12: Cospectral responses comparing the N_2O and temperature scalars for unstable (a) and stable (b) conditions. The similar behavior indicates real atmospheric structure that the N_2O sensor is observing.

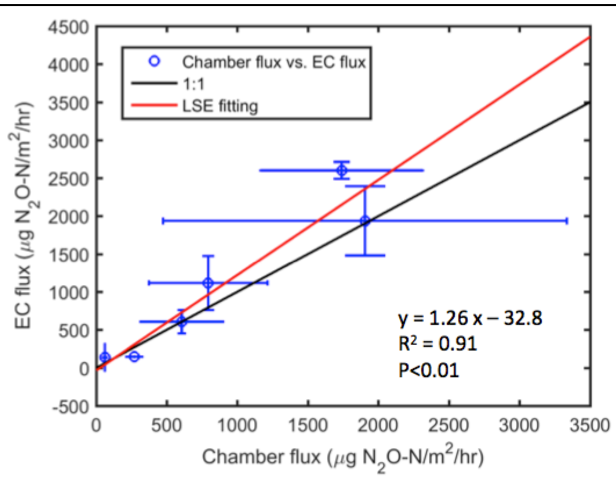

Figure 13: Comparison of the fluxes derived from the eddy covariance N_2O sensor and flux chambers within the tower footprint. Excellent correlation and agreement is observed within the space-time averaging differences.

Figure 13 shows an intercomparison where the eddy covariance fluxes were intercompared within the same time periods as a series of flux chamber measurements within the tower footprint at various days over the spring and summer. The EC fluxes from the N_2O sensor showed excellent correlation (r^2=0.91) with the chambers with the chamber fluxes over a range of values from 100-3000 μg N_2O-N m^{-2} hr^{-1}. The absolute magnitudes of the fluxes were also in excellent agreement with the EC fluxes, 26% higher than the chamber fluxes on average. Given the much different spatiotemporal timescales of the two methods, this agreement is very good.

Finally, the overall N_2O fluxes for both years showed strong diurnal trends. Figure 14 shows the 2015 (a) and 2016 (b) average fluxes binned by hourly increments. Highest fluxes were observed in the late afternoon and likely are the result of soil temperatures reaching their maximum. Relatively little fluxes were observed from midnight until well after sunrise. The fluxes in 2015 were much higher than 2016 due to a sampling bias of measurements themselves in 2015 (the month after fertilization and limited measurements thereafter due to detector problems). The 2016 data included longer lengths of time post fertilization and thus are much lower on average. Note that micrometeorological data from August 2016 onward are still undergoing final QC/QA along with the N_2O measurements and are not included on the 2016 plot. The strong diurnal variation of emissions, and seasonality of emissions (decreasing amounts after fertilization), show the high promise of deducing temporal emissions with the EC technique.

Overall, the high scientific value of N_2O eddy covariance measurements was demonstrated by the field tests including diurnal and seasonal flux variations, low detection limits (5 µg m^{-2} s^{-1}), and excellent agreement (26%) and correlation (r^2=0.91with chamber techniques.

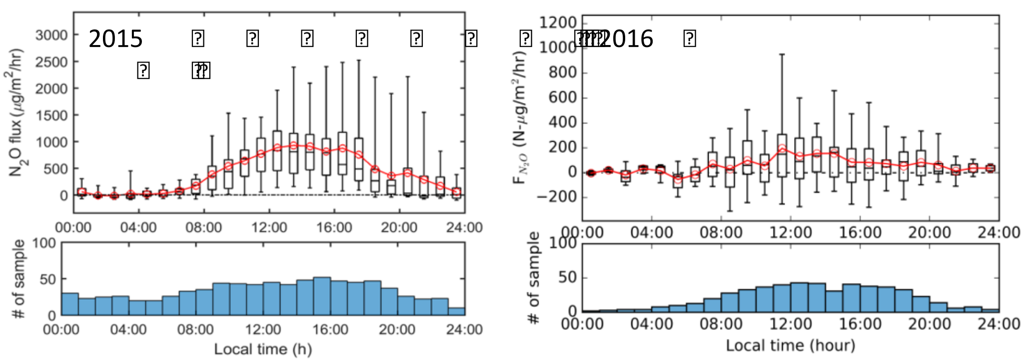

Figure 14: Diurnally-averaged N_2O fluxes over a corn field at KBS/MSU for 2015 and 2016. A strong daytime maximum in emissions is observed post-fertilization. Fluxes for 2016 are lower because the sampling period extended further into the summer after fertilization.

4. Summary of Results and Recommendations for Additional R&D

The Phase II results demonstrate the value of open path instrumentation for eddy covariance measurement of N_2O fluxes, and we were also able to demonstrate the efficacy of new low power interband cascade lasers for fast time response measurement of N_2O. These lasers will replace the power-hungry quantum cascade lasers as we further develop and commercialize this measurement technology. This latter breakthrough, made possible by the very recent commercial availability of room temperature ICLs in the 4.5 µm region, will enable the commercialization of truly portable N_2O flux instruments that have an exceedingly low power demand (5 – 10 watts). These instruments can be widely deployed at remote sites where the only power sources are solar power and batteries.

Future recommended development would build on these Phase II successes by production of four new prototype instruments, utilizing ICLs and implementing compact low power electronics designs. Three of these instruments would be used by our Princeton collaborators as well as external researchers to test and validate the instrumentation in field measurements of N_2O flux, including intercomparisons with other commercial instruments. Southwest Sciences would maintain one of the four prototypes in a laboratory setting in order to have it continuously available for further testing and refinement of the design. We would expect to incorporate any design changes needed to address feedback from the researchers (end users) who have tested the prototype in the field. Such feedback might include items such as user interface, interfacing to data acquisition systems (e.g. data loggers) typically used at field sites, improvement in calibration , maintenance procedures, etc. Our overriding goal is to refine and test the design of the instrumentation in order to make it ready for commercial manufacture and sale to the research community.

5. References

Baldocchi, D. et al., 2001, FLUXNET: A New Tool to Study the Temporal and Spatial Variability of Ecosystem–Scale Carbon Dioxide, Water Vapor, and Energy Flux Densities. *Bull. Amer. Meteor. Soc.*, **82**, 2415–2434

Butterbach-Bahl, K, Baggs E.M., Dannenmann, M, Kiese, R., and Zechmeister-Boltenstern, S., 2013, Nitrous oxide emissions from soils:how well do we understand the processes and their controls? Philosophical Transactions of the Royal Society B, **368**, 20130122, doi:10.1098/rstb.2013.0122

Hensen, A., Skiba, U., and Famulari, D., 2013, Low cost and state of the art methods to measure nitrous oxide emissions, Enviromental Research Letters, **8**, 025022, doi:10.1088/1748-9326/8/2/025022

Holland, E. A., Robertson, G.P., Greenberg, J., Groffman, P. M., Boone, R. D., and Gosz, J.R., 1999. Soil CO_2, N_2O, and CH_4 Exchange. [Robertson, G. P., Coleman, D. C., Bledsoe, C. S. (eds.)], Standard soil methods for long term ecological research, Oxford University Press, New York, New York, pp. 185-

IPCC, (2007) Climate Change 2007:The Physical Science Basis. Contribution of Working Group I to the Fourth Assessment Report of the Intergovernmental Panel on Climate Change [Solomon, S., D. Qin, M. Manning, Z. Chen, M. Marquis, K.B. Averyt, M.Tignor and H.L. Miller (eds.)], Cambridge University Press, Cambridge, United Kingdom and New York, NY, USA.

Migliavacca,M., *et al.* 2011, Semiempirical modeling of abiotic and biotic factors controlling ecosystem respiration across eddy covarian sites, Global Change Biology, **17**, 1, 390-409, doi:10.1111/j.1365-2486.2010.02243.x

Neftel, A., Ammann, C., Fischer, C., Spirig, C.,Conen, F., Emmenegger, L. Tuzson, B., and Wahlen, S., 2010, N_2O exchange over managed grassland:Application of a quantum cascade laser spectrometer for micrometeorological, Agricultural and Forest Meteorology, **150**, 775-785, doi:10.1016/j.agrformet.2009.07.013

Piao, S., *et al*. 2008, Net carbon dioxide losses of northern ecosystems in response to autumn warming, Nature, **451**, 49-52, doi:10.1038/nature06444

Ravishankara, A.R., Daniel, J.S., Portmann, R.W., 2009, Nitrous oxide (N_2O): The dominant ozone-depleting substance emitted in the 21st century, Science, 326, 123-125, doi:10.1126/science.1176985.

Reay, D.S., Davidson, E.A., Smith, K.A., Smith, P., Melillo, J.M., Dentener, F., and Crutzen P.J., 2012, Global agriculture and nitrous oxide emissions, Nature Climate Change, **2**, 410-416, doi:10.1038/nclimate1458

Ruan, L., and Robertson, G.P., 2013. Initial nitrous oxide, carbon dioxide and methane costs of converting Conservation Reserve Program land to row crops under conventional tillage vs. no-till. Global Change Biology, **19**, 2478-89, doi:10.1111/gcb.12216

Schwalm, C. R., *et al*.,2012, Reduction in carbon uptake during turn of the century drought in western North America, Nature Geoscience, **5**, 551-556, doi:10.1038/ngeo1529

Silver, J.A., 2005, Simple dense-pattern optical multipass cells, Applied Optics, **44**, 31, 6545-6556, doi:10.1364/AO.44.006545

Sun, K. L. Tao, L. Miller, D., Khan, M.A., Zondlo, M.A., 2013, Multi-Harmonic Inline Reference Cell for Optical Trace Gas Sensing in-line reference cell, patent pending, United States Patent and Trademark Office filed August 15, 2013. Application #61/683,536.

Sun, K., Tao, L., Miller, D.J., Khan, M.A., and Zondlo, M.A., 2012 Inline multi-harmonic calibration method for open-path atmospheric ammonia measurements, Applied Physics B-Lasers and Optics, **110**, 2, 213-222, doi:10.1007/s00340-012-5231-2

Tao, L., Sun, K., Khan, M.A., Miller, D. J., and Zondlo, M. A., 2012a, Compact and portable open-path sensor for simultaneous measurements of atmospheric N_2O and CO using a quantum cascade laser, Optics Express, **20**, 28106–28118, doi:10.1364/oe.20.028106

Vitousek, P. M., *et al*, 2009, Nutrient imbalances in agricultural development, Science, **324**, 5934,1519-1520, doi:10.1126/science.1170261

Zona, D., Janssens, I.A., Gioli, B., Jungkunst, H.F., Camino Serrano, M., Ceulemans, R., 2012. N_2O fluxes of a bio-energy poplar plantation during a two years rotation period. Global Change Biol. Bioenergy, 5, 5, 536-547, doi:10.1111/gcbb.12019

Zona, D., Janssens, I.A., Aubinet, M., Gioli, B., Vicca, S., Fichot, R., and Ceulemans, R., 2013, Fluxes of the greenhouse gases (CO_2, CH_4 and N_2O) above a short-rotation poplar plantation after conversion from agricultural land, Agricultural and Forest Meteorology, **169**, 100-110, doi:10.1016/j.agrformet.2012.10.008